

Systemic high-dose dexamethasone treatment may modulate the efficacy of intratumoral viral oncolytic immunotherapy in glioblastoma models

Marilyn S Koch ^{1,2}, Mykola Zdioruk,^{1,2} Michal O Nowicki,^{1,2} Alec M Griffith ^{2,3}, Estuardo Aguilar,⁴ Laura K Aguilar,⁴ Brian W Guzik,⁴ Francesca Barone,⁴ Paul P Tak,⁴ Ghazaleh Tabatabai,⁵ James A Lederer,^{2,3} E Antonio Chiocca,^{1,2} Sean Lawler^{1,2}

To cite: Koch MS, Zdioruk M, Nowicki MO, *et al*. Systemic high-dose dexamethasone treatment may modulate the efficacy of intratumoral viral oncolytic immunotherapy in glioblastoma models. *Journal for ImmunoTherapy of Cancer* 2022;**10**:e003368. doi:10.1136/jitc-2021-003368

► Additional supplemental material is published online only. To view, please visit the journal online (<http://dx.doi.org/10.1136/jitc-2021-003368>).

Accepted 23 November 2021



© Author(s) (or their employer(s)) 2022. Re-use permitted under CC BY-NC. No commercial re-use. See rights and permissions. Published by BMJ.

¹Department of Neurosurgery, Brigham and Women's Hospital, Boston, Massachusetts, USA

²Harvard Medical School, Boston, Massachusetts, USA

³Department of Surgery, Brigham and Women's Hospital, Boston, Massachusetts, USA

⁴Candel Therapeutics, Needham, Massachusetts, USA

⁵Department of Neurology and Interdisciplinary Neuro-Oncology, University Hospital Tuebingen, Tuebingen, Germany

Correspondence to

Sean Lawler;
slawler@bwh.harvard.edu

ABSTRACT

Background Intratumoral viral oncolytic immunotherapy is a promising new approach for the treatment of a variety of solid cancers. CAN-2409 is a replication-deficient adenovirus that delivers herpes simplex virus thymidine kinase to cancer cells, resulting in local conversion of ganciclovir or valacyclovir into a toxic metabolite. This leads to highly immunogenic cell death, followed by a local immune response against a variety of cancer neoantigens and, next, a systemic immune response against the injected tumor and uninjected distant metastases. CAN-2409 treatment has shown promising results in clinical studies in glioblastoma (GBM). Patients with GBM are usually given the corticosteroid dexamethasone to manage edema. Previous work has suggested that concurrent dexamethasone therapy may have a negative effect in patients treated with immune checkpoint inhibitors in patients with GBM. However, the effects of dexamethasone on the efficacy of CAN-2409 treatment have not been explored.

Methods In vitro experiments included cell viability and neurosphere T-cell killing assays. Effects of dexamethasone on CAN-2409 in vivo were examined using a syngeneic murine GBM model; survival was assessed according to Kaplan-Meier; analyses of tumor-infiltrating lymphocytes were performed with mass cytometry (CyTOF - cytometry by time-of-flight). Data were analyzed using a general linear model, with one-way analysis of variance followed by Dunnett's multiple comparison test, Kruskal-Wallis test, Dunn's multiple comparison test or statistical significance analysis of microarrays.

Results In a mouse model of GBM, we found that high doses of dexamethasone combined with CAN-2409 led to significantly reduced median survival (29.0 days) compared with CAN-2409 treatment alone (39.5 days). CyTOF analyses of tumor-infiltrating immune cells demonstrated potent immune stimulation induced by CAN-2409 treatment. These effects were diminished when high-dose dexamethasone was used. Functional immune cell characterization suggested increased immune cell exhaustion and tumor promoting profiles after dexamethasone treatment.

Conclusion Our data suggest that concurrent high-dose dexamethasone treatment may impair the efficacy

of oncolytic viral immunotherapy of GBM, supporting the notion that dexamethasone use should be balanced between symptom control and impact on the therapeutic outcome.

BACKGROUND

Glioblastoma (GBM) is the most common malignant primary brain tumor, and patient survival remains poor despite multimodal standard therapy consisting of maximum surgical resection and concomitant radio-chemotherapy.¹ Many novel therapeutic approaches that are being explored in cancer are focused on harnessing the patient's immune system to target tumor cells. These include immune checkpoint inhibition,² vaccines against tumor antigens,³ chimeric antigen receptor (CAR) T-cell therapies,⁴ intratumoral viral oncolytic immunotherapies,^{5,6} and small molecule immune stimulatory ligands.⁷

GBM is characterized by abnormal angiogenesis and disruption of the blood-brain barrier, often resulting in cerebral edema, which can cause significant morbidity. This may necessitate antiedema therapy using dexamethasone, which suppresses the patient's immune system.⁸ In comparison to other corticosteroids, dexamethasone shows greater potency, a prolonged half-life, reduced mineral corticoid activity and good brain penetration.⁹ The effects of dexamethasone on malignant glioma cell growth and patient survival have remained controversial, and evidence of efficacy or optimal dosing is scarce.

Until now, studies have mainly examined the influence of corticosteroids on the efficacy of standard of care (SOC) in GBM. Retrospective analyses revealed compromised

survival in patients with higher dexamethasone treatment.^{10–11} Under treatment with tumor-treating fields, dexamethasone significantly shortened overall survival in a dose-dependent manner.¹² In recent human immunotherapy trials, dexamethasone treatment was associated with reduced survival⁵ and tumor-infiltrating lymphocyte (TIL) responses against cognate peptide antigen.¹³ Steroid use limited survival in the context of systemic immune checkpoint blockade in mouse models of GBM.¹⁴ It has also been suggested that dexamethasone may have a negative impact on the response to immune checkpoint inhibitor treatment in patients with GBM.¹⁵ Effects of dexamethasone have been shown to reduce the potency of an oncolytic adenovirus,¹⁶ but despite its frequent concurrent use, the effects of dexamethasone on local intratumorally administered viral immunotherapies have not been examined thoroughly in the context of GBM.

CAN-2409 is a non-replicating serotype 5 adenovirus expressing the herpes simplex virus thymidine kinase (HSV-TK) gene. Intratumoral injection of CAN-2409 is combined with a course of systemic treatment with ganciclovir (GCV) or valacyclovir to induce both immunogenic tumor cell death and a local immune response against the tumor, followed by a systemic immune response.^{15–17–18} CAN-2409 treatment is currently being evaluated in clinical trials in various solid tumors, including GBM. Previous work has shown encouraging survival data in a phase II study in newly diagnosed patients with GBM undergoing SOC.⁶

This study sought to investigate the impact of high-dose dexamethasone treatment on the effectiveness of local immunotherapies, using CAN-2409 treatment as a model. First, we examined the effects of dexamethasone on T-cell responses against tumor cells exposed to CAN-2409 in vitro using coculture assays. Next, we used immunocompetent murine GBM models to evaluate the effects of high-dose dexamethasone and observed a negative effect of high-dose dexamethasone treatment on survival in mice treated with CAN-2409. Our data support the view that dexamethasone use should be limited to maximize the potential for immunotherapies in GBM.

MATERIALS AND METHODS

Cell culture and reagents

For in vitro experiments, we used the patient-derived GBM stem-like cell line G9_pCDH¹⁹ with Neurobasal Medium (Life Technologies) containing B27 (Invitrogen), 1% Glutamax (Invitrogen), 20 ng/mL epidermal growth factor (EGF) (Peprotech), 20 ng/mL fibroblast growth factor (FGF) (Peprotech), Primocin (Invivogen) and Plasmocin (Invivogen), and the GBM cell lines U1242_LRP and U87_GFP cultured in Dulbecco's modified Eagle's Medium (Life Technologies), containing 10% heat-inactivated fetal bovine serum, Plasmocin and Primocin. For in vivo studies, GL261fluc cells were used (PerkinElmer). U1242 was a kind gift from James van

Brooklyn²⁰ and U87 was purchased from American Type Culture Collection (ATCC). All cells were cultured at 37°C, 5% CO₂. Cells were regularly PCR-tested for mycoplasma infection. GCV and CAN-2409²¹ were provided by Candel Therapeutics. For the in vitro experiments, cells were treated with CAN-2409 (MOI 100–500), GCV (10 µg/mL) and dexamethasone (West-Ward, 1–10 µM).

Cell viability assays

Cells were seeded in quintuplicate at 5000 cells/well in 96-well plates and treated as indicated. PrestoBlue cell viability agent (Life Science Technologies) was added 96 hours after seeding, and measured with an OmegaStar plate reader (BMG Labtech).

PBMC and CD8⁺ T-cell preparation

Peripheral blood mononuclear cells (PBMCs) were acquired from healthy donor blood using the Ficoll-Paque PLUS gradient method (GE Healthcare). CD8⁺ T cells were isolated from PBMCs with the CD8⁺ T Cell Isolation Kit, human (Miltenyi Biotec) and activated using 1:1 Dynabeads Human T-Activator CD3/CD28 for T Cell Expansion and Activation (Gibco) and human interleukin (IL)-2 at 10 ng/mL (Peprotech).

T-cell killing assays

A single cell suspension of GBM cells was seeded at 750 cells/well (G9_pCDH, U87_GFP, U1242_LRP) in triplicate or quintuplicate in ultralow-attachment 96-well plates (Corning) and incubated for 48 hours to allow sphere formation. CD8⁺ T cells were added together with the indicated therapies. For the T-cell killing assays with IL-12, 10 ng/mL of human recombinant IL-12 (R&D Systems) was added. Cells were incubated for another 6 days. Microscope images of the spheres were taken daily (Nikon TI, ×4 magnification), and the sphere area was measured using ImageJ.

Animal studies

For the survival study, female albino C57/BL6 mice 7–8 weeks old were purchased from Envigo. A total of 100 000 GL261fluc cells were injected intracranially in 2 µL Hanks' balanced salt solution (HBSS) 2 mm right lateral, 1 mm frontal to the bregma, and 3 mm deep. Nine days later, 3 µL of CAN-2409 (2 × 10⁸ vector particles/µL) respectively sham were injected into the same location. GCV (20 mg/kg bodyweight) was administered two times per day, and dexamethasone (10 mg/kg bodyweight) once per day intraperitoneally for a total of 7 days. Control cohort animals did not receive any treatment. Successful tumor implantation was verified by bioluminescence imaging using the PerkinElmer IVIS Lumina 3. Each cohort consisted of 6 animals (total: 24 animals). Animals were distributed to the separate groups based on bioluminescence signal and body weight and were treated in the same session, and located in the same space in adjacent cages. The study endpoint was considered as a weight loss of 20%, onset of neurological symptoms, or signs of pain and distress. For the generation of

TILs, animals 13–14 weeks old of the same strain underwent the same aforementioned procedures; to optimize the immune cell yield, the injection of CAN-2409 was performed 7 days after tumor implantation. All animal experiments and procedures described in this study were approved by Brigham and Women's Institutional Animal Care and Use Committee. Animals' sample size was determined with the resource equation method.²²

MRI

For the purpose of MRI, mice were anaesthetized with isoflurane and MRI was performed using a BioSpec 3T (Bruker). The set-up 'mouse body RF coil with respiratory monitoring' was used. Images were acquired using the T2_TurboRARE sequence with the following settings: echo time: 47.73 ms, repetition time: 4993.715 ms, Rare Factor: 8, Averages: 3. Slice thickness: 0.5 mm, slicer orientation: axial. Field of View: 20 mm×20 mm, Resolution: 0.078 mm×0.078 mm. Images were extracted using the Horos open source medical image viewer V.3.3.6, tumor volume was analyzed with the JiveX DICOM viewer (VISUS Health IT GmbH, Bochum, Germany).

Isolation of murine tumor-infiltrating leukocytes

The tumor-bearing right hemisphere was collected from each mouse on day 20 after tumor implantation. Each treatment cohort consisted of 4 animals (total: 16). A tumor dissociation kit for mouse (Miltenyi Biotec) was used for isolation of tumor infiltrating leukocytes according to the manufacturer's instructions. Harvested leukocytes were stored at -80°C until further use.

Mass cytometry (CyTOF)

All samples were thawed in a 37°C water bath and mixed with thawing media containing RPMI Medium 1640 (Life Technologies) supplemented with 5% heat-inactivated fetal bovine serum (Life Technologies), GlutaMAX (Life Technologies), antibiotic–antimycotic (Life Technologies), Minimum Essential Media (MEM) non-essential amino acids (Life Technologies), HEPES (4-(2-hydroxyethyl)-1-piperazineethanesulfonic acid) (Life Technologies), 2-mercaptoethanol (Sigma-Aldrich), sodium heparin (Sigma-Aldrich), and benzonase nuclease (Sigma-Aldrich). Aliquots of each sample post-thaw were mixed with PBS (Life Technologies) at a 1:1 ratio to be counted by flow cytometry. Between 0.5 and 2.0×10^6 cells were used for each sample. The samples were spun down and aspirated. Cisplatin viability staining reagent (Fluidigm) was added. Samples were fixed with 0.2% formaldehyde before staining. After centrifugation, mouse anti-CD16/32 antibody Fc-receptor blocking reagent (BioLegend) was used in cell staining buffer (CSB) (PBS with BSA (Sigma Aldrich) and sodium azide (Sigma Aldrich)) for 15 min followed by incubation with conjugated surface antibodies (each marker was used at a 1:100 dilution in CSB, unless stated otherwise) for 30 min. Samples were stained (see online supplemental figure 5 for used markers), CD115, PD-1 and vascular endothelial

growth factor receptor (VEGFR) were not detectable. All antibodies were obtained from the Harvard Medical Area CyTOF Antibody Resource and Core (Boston, Massachusetts, USA).

Samples were fixed with 4% formaldehyde before permeabilization with the FoxP3/Transcription Factor Staining Buffer Set (ThermoFisher Scientific) and were incubated with SCN (thiocyanate)–EDTA-coupled palladium-based barcoding reagents for 15 min and then combined into a single sample. Samples were incubated in a heparin solution for 15 min. Conjugated intracellular antibodies (each marker was used at a 1:100 dilution in permeabilization buffer, unless stated otherwise) were added into each tube and incubated for 60 min. Cells were then fixed with 4% formaldehyde for 10 min.

To identify single cell events, DNA was labeled for 20 min with an iridium intercalator solution (Fluidigm). Samples were subsequently washed and reconstituted in Maxpar Cell Acquisition Solution (Fluidigm) in the presence of EQ Four Element Calibration beads (Fluidigm) at a final concentration of 1×10^6 cells/mL. Samples were acquired on a Helios CyTOF Mass Cytometer (Fluidigm). Raw FCS files were normalized to reduce signal deviation over time, using the bead standard normalization method established by Fink *et al.*²³ The normalized files were then compensated with a panel-specific spillover matrix to subtract cross-contaminating signals, using the CyTOF-based compensation method.²⁴ These compensated files were then deconvoluted into individual sample files using a single-cell-based debarcoding algorithm.²⁵ Files were uploaded to OMIQ. In OMIQ, events were cleaned up using Gaussian parameters and then gated to remove normalization beads and to select live singlets. The latter were run through a principal component analysis for pre-embedding for an opt-SNE dimensionality reduction.²⁶ From there, events were clustered using PARC²⁷ to identify populations based on marker expression. Statistically different clusters between groups were identified using the multiclass setting of significance analysis of microarrays (SAM),²⁸ followed by statistical testing with Kruskal-Wallis rank-sum test with Dunn's multiple comparison; p values were adjusted with the Benjamini-Hochberg method. Differences in the separate leukocyte populations after treatment were assessed using a general linear model (GLM). For this, cell counts by group were exported and analyzed in the R package edgeR using the quasi-likelihood negative binomial generalized log-linear model. This was performed using the functions estimateDisp for dispersion estimation, glmQLFit to fit to the GLM, and glmQLFTest to run F-Tests on the fitted model.

Statistics

All statistical analyses were performed with GraphPad Prism V.8.3.0. One-way analysis of variance (ANOVA) with Dunnett's multiple comparison's test was applied for statistical testing for neurosphere assays and statistical testing with a GLM and non-parametric Kruskal-Wallis test with Dunn's multiple comparison test for

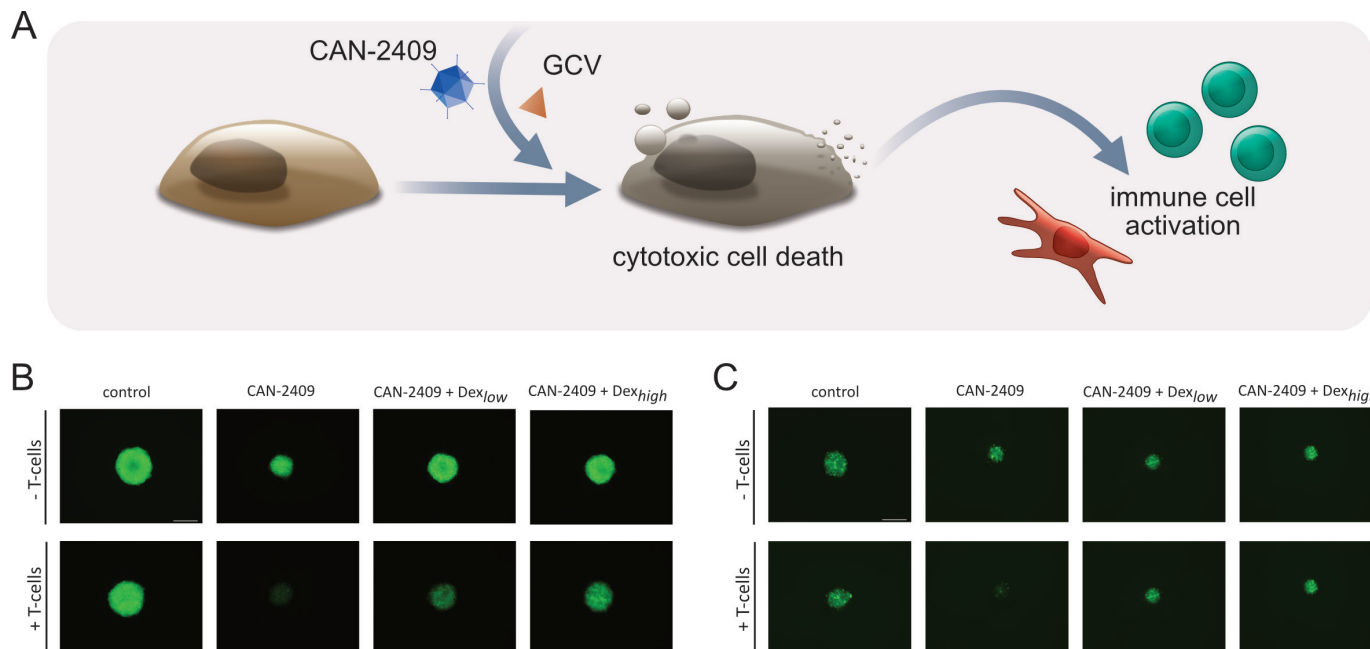


Figure 1 Dexamethasone interferes with CAN-2409/GCV cytotoxic and immunogenic effect. (A) Mechanism of CAN-2409/GCV. After intratumoral injection of CAN-2409, HSV-TK is expressed in tumor cells and metabolizes the administered prodrug GCV, inducing DNA damage. This results in (1) apoptotic and necrotic tumor cell death and hence leads to (2) immune cell activation. (B,C) Dexamethasone reduces the immunogenic effect of CAN-2409/GCV. For T-cell killing assays, G9_pCDH (B,C) and U87_GFP (D,E) were cocultured with either activated CD8⁺ T cells, CAN-2409/GCV, dexamethasone 1 μM/10 μM or the combination as indicated and imaged daily for 6 days. Sphere area was normalized to sphere size on day 0. Images on day 5 show a smaller sphere size between CAN-2409/GCV and combination of both ±CD8⁺ T cells. Addition of CD8⁺ T cells is associated with reduced sphere size and fluorescence intensity (×4 magnification, scale bar=500 μm). GCV, ganciclovir.

comparison of leukocyte population abundance. Leukocyte subcluster comparison was analyzed with two-way ANOVA and Dunnett's multiple comparison's test. For analysis of survival outcomes, data were analyzed according to Kaplan-Meier; comparison of survival curves was performed with the log-rank test. Significance is indicated with asterisks.

RESULTS

Dexamethasone attenuates suicide gene therapy mediated by CAN-2409/GCV cytotoxicity in vitro

CAN-2409 is a non-replicating adenovirus expressing the HSV-TK gene. After intratumoral injection of CAN-2409 in vivo, systemic treatment with GCV results in the formation of a toxic metabolite, a nucleotide analog, under the influence of local expression of HSV-TK (figure 1A). At the same time, the adenoviral serotype 5 capsid protein will induce a strong proinflammatory response as a result of upregulation of proinflammatory cytokines, adhesion molecules and chemokines.²⁹ Together, these effects induce a specific T-cell response against the injected tumor and uninjected metastases.^{30 31}

We wanted to determine if dexamethasone could limit the activation of T cells against tumor cells exposed to a cytotoxic stimulus in vitro, as has been shown, for example, with radiation-induced toxicity. To test this, we performed 3D cell proliferation assays with CAN-2409/GCV in GBM neurosphere models with patient-derived

GBM cells (G9_pCDH, figure 1B and online supplemental figure 1C) and an established cell line (U87_GFP, figure 1C and online supplemental figure 1C) in the presence or absence of T cells.

In the absence of T cells, dexamethasone at high doses (10 μM/DEX_{high}) was associated with a small but significant increase in tumor sphere area compared with CAN-2409/GCV monotherapy in both cell lines (CAN-2409/GCV vs CAN-2409/GCV +DEX_{high}, p=0.001–0.187), while the lower dose (1 μM/DEX_{low}) did not seem to have a consistent relevant impact (CAN-2409/GCV vs CAN-2409/GCV+DEX_{low}, p=0.004–0.026, with 66% of all assays being not statistically significant). CAN-2409/GCV in combination with activated CD8⁺ T cells led to further enhancement of cell killing, and dexamethasone significantly abrogated this effect, increasing the sphere area at low and high doses in the patient-derived G9 GBM cell line (CAN-2409/GCV vs CAN-2409/GCV+DEX_{low}, p=ns–0.008; CAN-2409/GCV vs CAN-2409/GCV +DEX_{high}, p<0.02–0.0007), whereas in the U87 neurospheres, this was only the case at higher doses (CAN-2409/GCV vs CAN-2409/GCV +DEX_{low}, ns, CAN-2409/GCV vs CAN-2409/GCV +DEX_{high}, p=ns–0.008) (data not shown). These data show that GBM sphere growth with T cells in the presence of dexamethasone closely resembles its effects in the absence of T cells, suggesting an almost complete abrogation of the additional immune-mediated effect of CAN-2409/GCV by dexamethasone, particularly in the patient-derived G9 cell line.

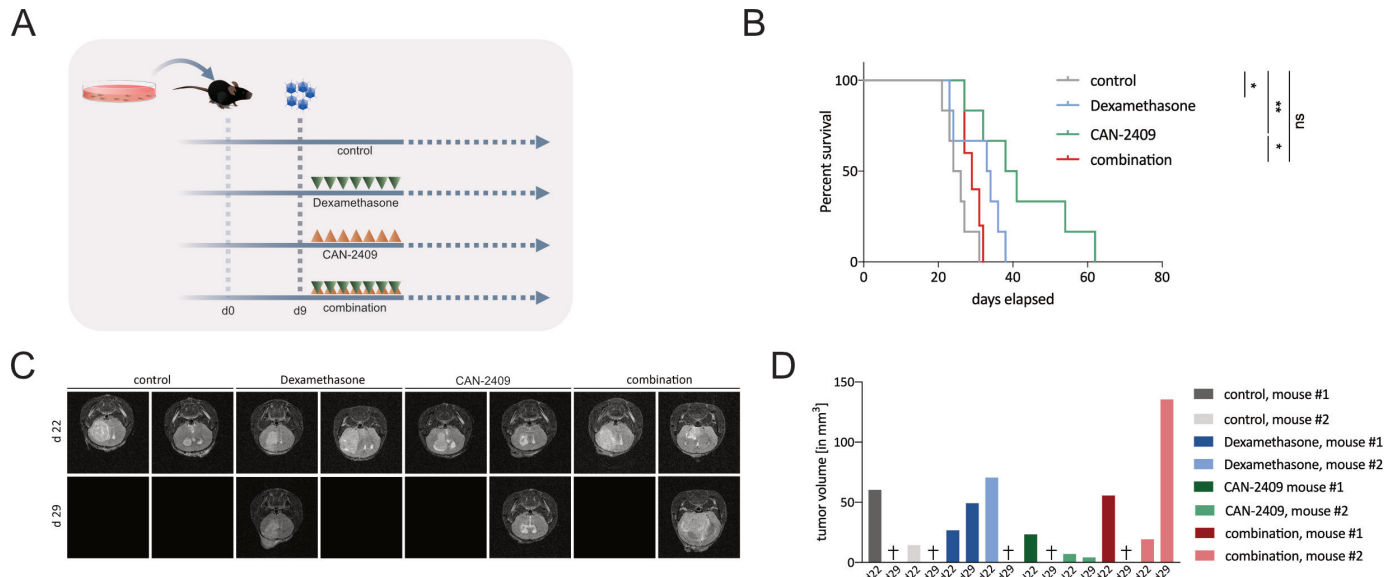


Figure 2 Dexamethasone blocks responses to CAN-2409 in vivo. (A) Experimental set-up in vivo. A total of 100 000 GL261fluc cells were injected intracranially in the right hemisphere; 9 days after tumor implantation, CAN-2409 was injected at the same location, followed 24 hours later by daily GCV (group AdV-tk +GCV) and/or dexamethasone (group combination) treatment for a total of 7 days. Each cohort n=6. (B) Kaplan-Meier survival curves. While treatment with CAN-2409 (39.5 days) and dexamethasone (33.5 days) alone led to a significant longer median survival compared with control (25 days) (CAN-2409 vs control, log-rank test: $p=0.0022$; dexamethasone vs control, $p=0.0386$), the combination resulted in significant reduction of the CAN-2409-effect (combination vs CAN-2409, log-rank test: $p=0.0184$) and was not statistically different compared with control (combination vs control, log-rank test: ns). Curves were right-censored on day 86. One outlier animal from the control group was excluded from the study because it did not display any evidence of lasting successful tumor formation by immunostaining (online supplemental figure S3) and was therefore excluded from the analysis. (C) MRI. Representative T2 -weighed magnetic resonance images 22 and 29 days after tumor implantation from animals of the survival study (B). All animals ($n=2$ /group) displayed tumor formation on day 22. On day 29, five animals had reached endpoint and therefore images are blank. Among the surviving animals on day 29, the tumor volume in the CAN-2409-treated animal was less, whereas the tumor in the dexamethasone and the combination-treated animal had increased. (D) Tumor volumetry. Tumor volume per animal of days 22 and 29. Animals that had reached endpoint on day 29 are marked with (+). GCV, ganciclovir; ns, not significant.

These data show that CAN-2409/GCV potently stimulates the tumor cell killing ability of T cells and that dexamethasone, especially at higher doses, could attenuate these immunogenic effects.

Concurrent use of high-dose dexamethasone blocks the pro-survival effects of CAN-2409 in vivo

Based on its mechanism of action as described previously, the immunogenic effect of CAN-2409 treatment can only be properly studied in in vivo models. Tumor cell death mediated by HSV-TK has been shown to induce apoptotic and necrotic cell death,^{17 18} as well as potent immune stimulation in vivo.¹⁷ Dexamethasone may impede inflammatory responses in experimental glioma models.^{14 32} To evaluate the impact of dexamethasone on efficacy of CAN-2409 treatment, in vivo studies were carried out in C57/Bl6 mice using the syngeneic immunocompetent GL261 GBM cell line (figure 2A). The non-treated control cohort had the shortest median survival time (25 days), and CAN-2409-treated animals lived longest (39.5 days, log-rank test: control vs CAN-2409, $p=0.002$), followed by dexamethasone only (33.5 days, control vs DEX $p=0.038$) and CAN-2409/DEX combination (29 days, log-rank test: control vs combination, $p=0.078$). Addition of high-dose dexamethasone significantly reduced survival when

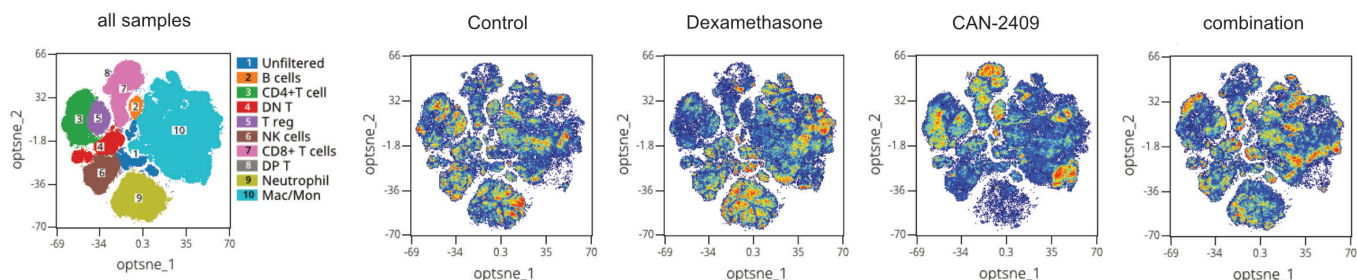
compared with CAN-2409 alone (log-rank test CAN-2409 vs combination, $p=0.018$) (figure 2B).

To visualize the dynamics of tumor development, MRI was performed on two animals per group on days 22 and 29 after tumor implantation (figure 2C). All animals showed detectable tumor on day 22. On day 29, five of the eight animals that underwent MRI had reached their endpoint.

High-dose dexamethasone markedly alters the tumor immune microenvironment and reduces CAN-2409-mediated immune stimulatory effects

To determine the impact of CAN-2409 and dexamethasone on immune cells, mass cytometry (CyTOF) analyses were performed 10 days post-treatment using the GL261 murine GBM model. Twenty-nine cell clusters with distinct marker expression were identified (online supplemental figure S4,5). The composite tSNE overlay map (figure 3A) illustrates all immune cell subsets identified in tumors as well as the relative differences in cell subset densities between control and the different treatment groups. Compared with controls, the CAN-2409-associated distribution of immune cells shows changes associated with its antitumor effects, including relative decreases in macrophages, regulatory T cells (Tregs),

A



B

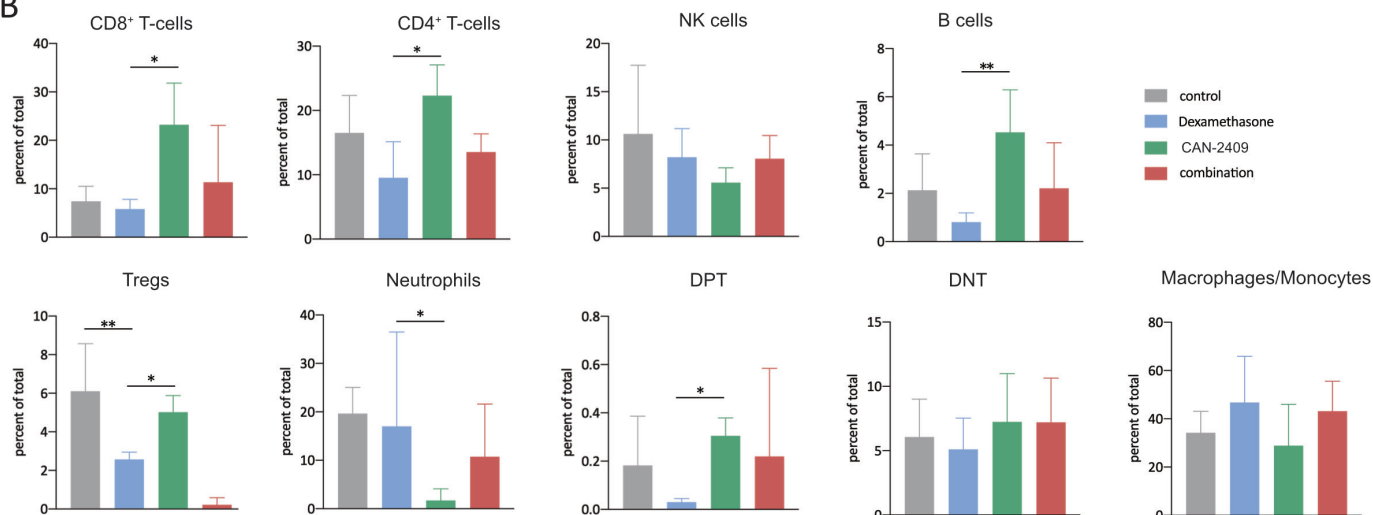


Figure 3 Altered CAN-2409-induced tumor microenvironment after DEX. (A) tSNE plots of all samples and single therapies. tSNE plots displaying immune cell subset identification overlay plots and density dot plots of CyTOF-analyzed murine tumor infiltrating leukocytes. (B) Therapy-related alteration of leukocyte populations. Percentages of total cell populations are displayed. CAN-2409 increases the percentages of CD8⁺, CD4⁺, B-cell, Treg and DPT cell populations, whereas combinatorial treatment is associated with a reduction of these populations and an increase in NK cells, neutrophils, and macrophages. Testing with GLM showed significant reduction of CD8⁺ ($p=0.016$), CD4⁺ ($p=0.02$) T cells, B cells ($p=0.01$), and DPT cells ($p=0.02$) as well as an increase of neutrophils ($p=0.02$) after DEX treatment compared with CAN-2409, and a significant reduction of Tregs after DEX treatment compared with control and CAN-2409 ($p=0.01$ resp. $p=0.016$) (bars show mean \pm SD). t-SNE, t-distributed stochastic neighbor embedding; DEX, dexamethasone; DNT, double negative T; DPT, double positive T; GLM, general linear model; NK, natural killer; tSNE, t-distributed stochastic neighbor embedding.

natural killer (NK) cells and neutrophils and increases in T cells, B cells, and double positive T (DPT cells, expressing both CD4 and CD8) compared with controls (figure 3B).

As proven by a GLM analysis, CAN-2409 led to a nearly significant trend compared with control for CD8⁺ T cells (adj. $p=0.051$) and neutrophils (adj. $p=0.051$). Dexamethasone in comparison to CAN-2409 led to a significant decrease of CD8⁺ and CD4⁺ T cells, DPT cells, B cells and Tregs and a significant increase of neutrophils (online supplemental figure 7). Combination treatment partially reversed the immunostimulatory effects of CAN-2409, showing increases in macrophages, NK cells and neutrophils as well as a corresponding reduction of CD4⁺ and CD8⁺ T cells, B cells, Tregs and DPTs compared with CAN-2409 alone (figure 3A,B), although not being statistically significant with the number of samples used.

The most significant changes were seen in Tregs, the proportion of which did not greatly change after CAN-2409 treatment, but they were significantly reduced by

high-dose dexamethasone treatment alone and even further after the combination treatment as revealed by complimentary testing with one-way ANOVA and consecutive Dunnett's multiple comparison test (control vs combination, $p=0.0001$; control vs dexamethasone, $p=0.007$).

Taken together, these observations show that CAN-2409 treatment creates a comparatively 'hot' tumor microenvironment and a T-cell response against the tumor, while high-dose dexamethasone treatment causes the opposite, with global changes across immune cells. In line with this, our data collectively show that the effects of CAN-2409 treatment on immune cell infiltrates are partially inhibited by concurrent treatment with high-dose dexamethasone.

High-dose dexamethasone treatment induces exhaustion and reduces T-cell activation marker expression induced by CAN-2409 treatment

Three CD8⁺ and two CD4⁺ T-cell clusters were identified in the CyTOF data and were analyzed by the

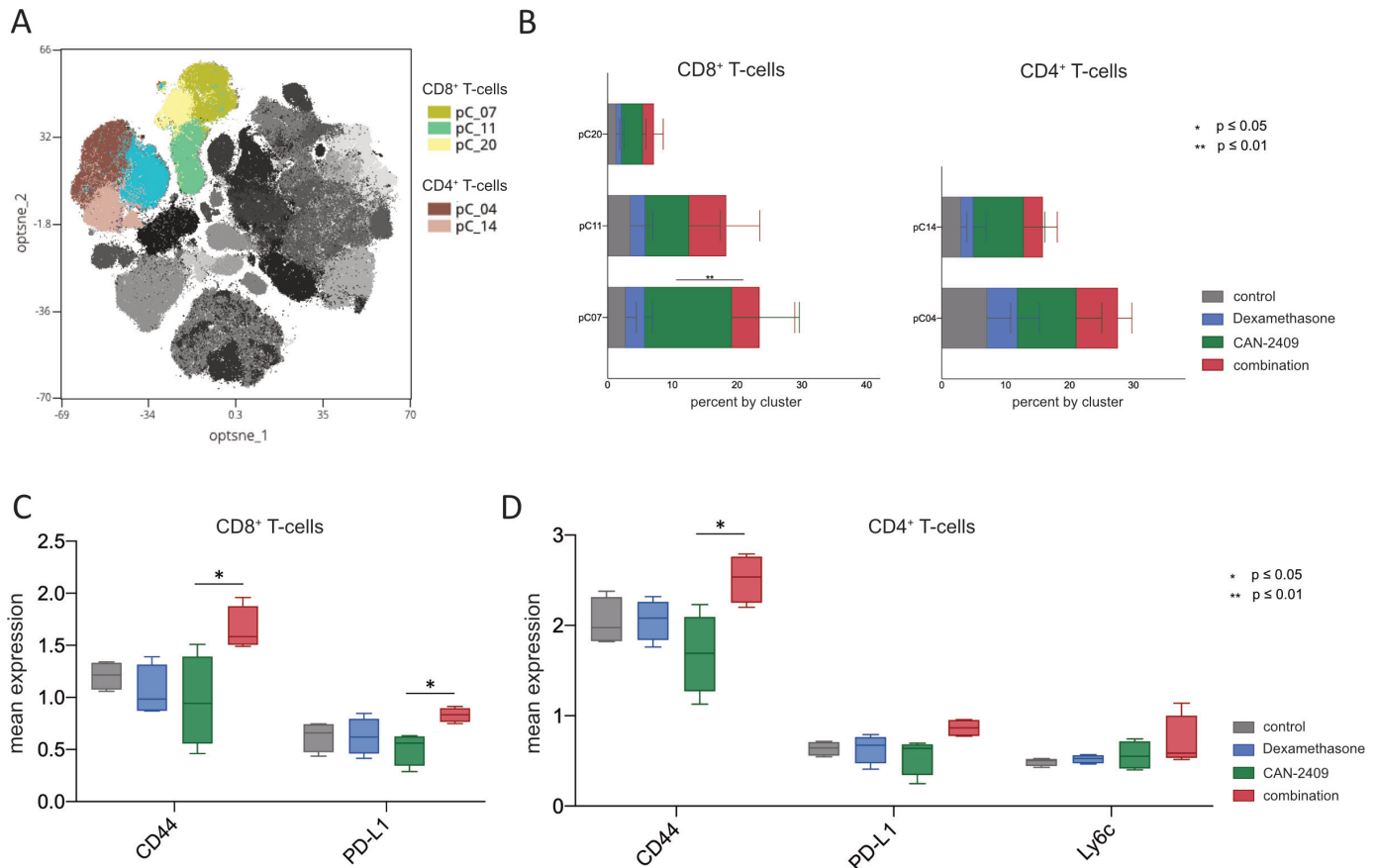


Figure 4 Treatment with dexamethasone \pm CAN-2409 affects T-cell profiles. (A) Overlay of leukocyte clusters on tSNE plot with focus on T cells. Cluster of interest for CD8⁺ T cells are pC07, 11, and 20, and for CD4⁺ T cells pC04 and 14. (B) Cluster distribution within CD8⁺ and CD4⁺ T cells in relation to therapy. CD8⁺ and CD4⁺ T cells consist of indicated clusters. Predominant cluster throughout all treatment groups is pC07 for CD8⁺ and pC04 for CD4⁺ T cells. CAN-2409 leads to increased cell abundance among all clusters, whereas dexamethasone and the combination therapy induces the opposite effect. This effect is statistically significant in pC07 ($p=0.0084$) (bars show mean \pm SD). (C,D) Expression of significantly altered markers on CD8⁺ and CD4⁺ T cells. Graphs display the median expression of CD44 and PD-L1 without or after treatment with dexamethasone, CAN-2409 and the combination on CD8⁺ (C) and the median expression of CD44, I-A/I-E, CD39, PD-L1, CD152 and Ly6C on CD4⁺ T cells (D). Combination treatment is associated with increased expression of CD44, PD-L1, I-A/I-E, CD39 and Ly6C compared with CAN-2409, with CD44 (p adj.=0.045) and PD-L1 (p adj.=0.045) being significantly upregulated in the combination treatment for CD8⁺ cells and CD44 being significantly upregulated in CD4⁺ cells (p adj.=0.028). PD-L1, programmed death-ligand 1.

PARC (phenotyping by accelerated refined community-partitioning) clustering algorithm²⁷ (figure 4A). Cluster abundance analysis is shown (figure 4) to visualize treatment effects on CD8⁺ T cell clusters pC07, pC11 and pC20; CAN-2409 treatment increased the proportion of all these clusters, which was statistically significant in the case of pC07, the most prevalent cluster observed after CAN-2409 treatment. High-dose dexamethasone treatment partially suppressed the increase in the pC07 CD8⁺ T-cell cluster.

Detailed marker analysis of the CD8⁺ T-cell clusters showed that the pC07 cluster, which was strongly induced by CAN-2409 treatment, was distinguished by elevated levels of granzyme B, CD38 and CD69, indicating an activated effector T-cell phenotype, which is potentially counterbalanced in this cluster by increased levels of the suppressive markers CD152 (CTLA4) and CD39 (online supplemental figure S4). The less abundant pC11 and pC20 CD8⁺ T-cell

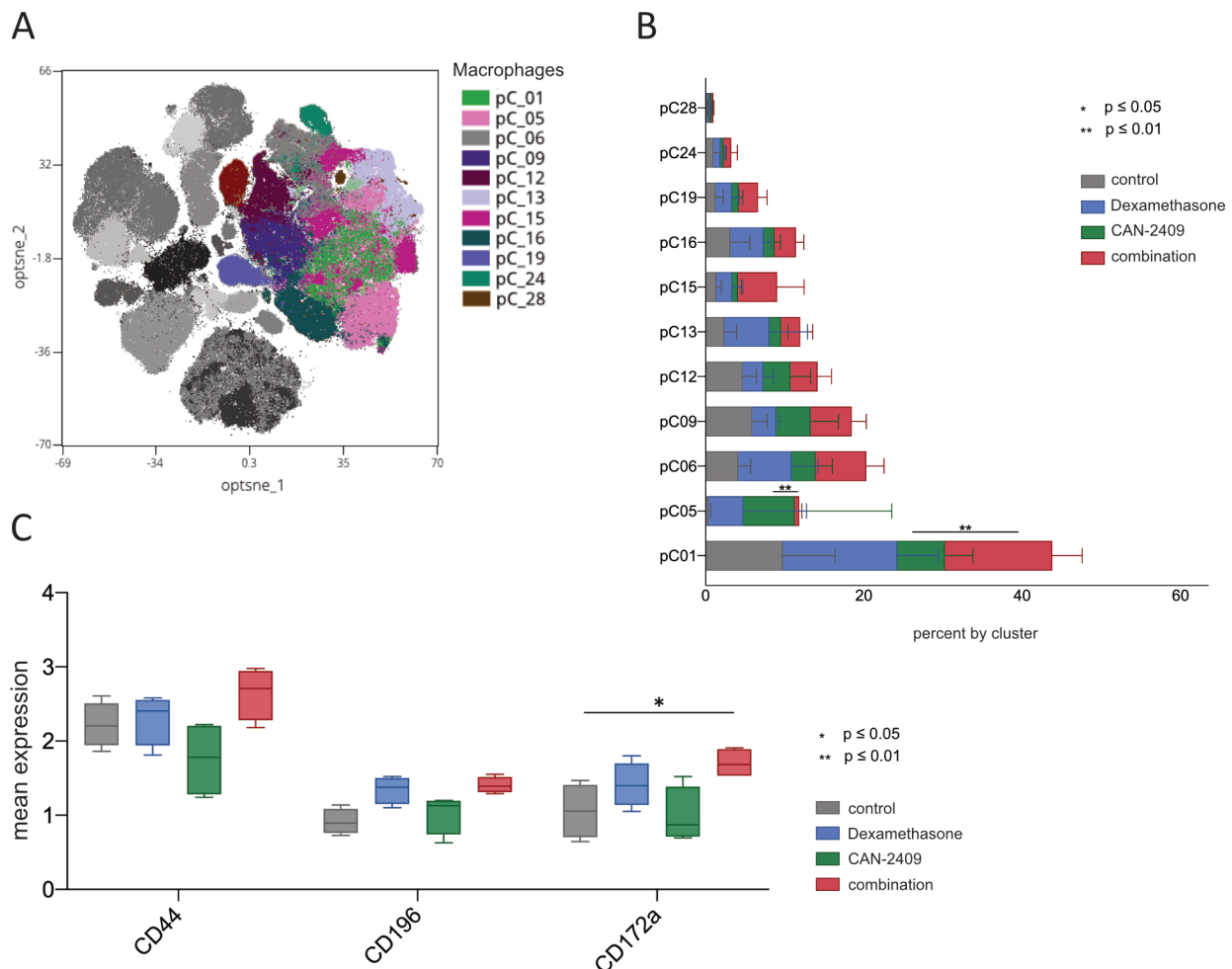
clusters express multiple activation markers, indicating T-cell effector function, but did not show increased levels of CTLA4 and CD39. The pC07 and pC11 clusters are also characterized by the IL-27/IFN γ -stimulated Ly6C effector T-cell marker (online supplemental figure S4). Although pC20 does not show high Ly6C, the increased expression of CD86, CD69 in all three clusters is consistent with type I interferon-induced memory or effector T cells.³³

CD4⁺ T cells were primarily clustered as pC14 and pC04 and show a similar pattern of CAN-2409 treatment-induced increase and repression by high-dose dexamethasone (figure 4B). The CD4⁺ dominating cluster pC04 differs from pC14 by expression of CD73, CD39, CD86 and CD69, with CD73 and CD39 pointing to a regulatory function,³⁴ while CD69 acts as a marker of early T-cell activation,³⁵ and CD86 has been shown to be expressed on memory effector T cells³⁶ (online supplemental figure S4).

To evaluate relevant shifts in the expression of individual markers on specific cell types, statistical SAM, followed by testing with Kruskal-Wallis rank-sum test with Dunn's multiple comparison, was performed. High-dose dexamethasone and the high-dose dexamethasone/CAN-2409 combination treatment led to upregulation of CD44 and programmed death-ligand 1 (PD-L1) on CD8⁺ T cells (figure 4C) and of CD44, Ly6C, CD39, I-A/I-E and PD-L1 on CD4⁺ T cells compared with controls and single treatments (figure 4D). These changes indicate a shift to an immunosuppressive micro-environment by dexamethasone denoted by CD152/CTLA-4 and PD-L1. CTLA-4 upregulation could mirror a more exhausted cell state in the combination treatment versus CAN-2409. PD-L1 expression on T cells has also been shown to suggest a less favorable immunogenic profile.^{37–39}

Proinflammatory effects of CAN-2409 on innate immune cells are suppressed by dexamethasone

Alterations in the treatment groups manifested across a range of innate immune cells. As shown in figure 3, dexamethasone treatment tended to increase the proportion of tumor-infiltrating macrophages, which is maintained in the presence of CAN-2409 treatment. Clustering identified a total of nine macrophage clusters (figure 5A). To interrogate this in greater detail, we examined the effects of CAN-2409 and high-dose dexamethasone treatment on each cluster. CAN-2409 had little effect on the proportion of infiltrating cells in the predominant cluster pC01 (figure 5B). In contrast, dexamethasone caused a significant increase as compared with CAN-2409 treatment. Marker analysis showed that pC01 shares some features of tumor-promoting macrophages, positive for CD11b, F4/80, and CD68 as well as the suppressive markers CD206, PD-L1, CD39, and Arg-1 (online supplemental



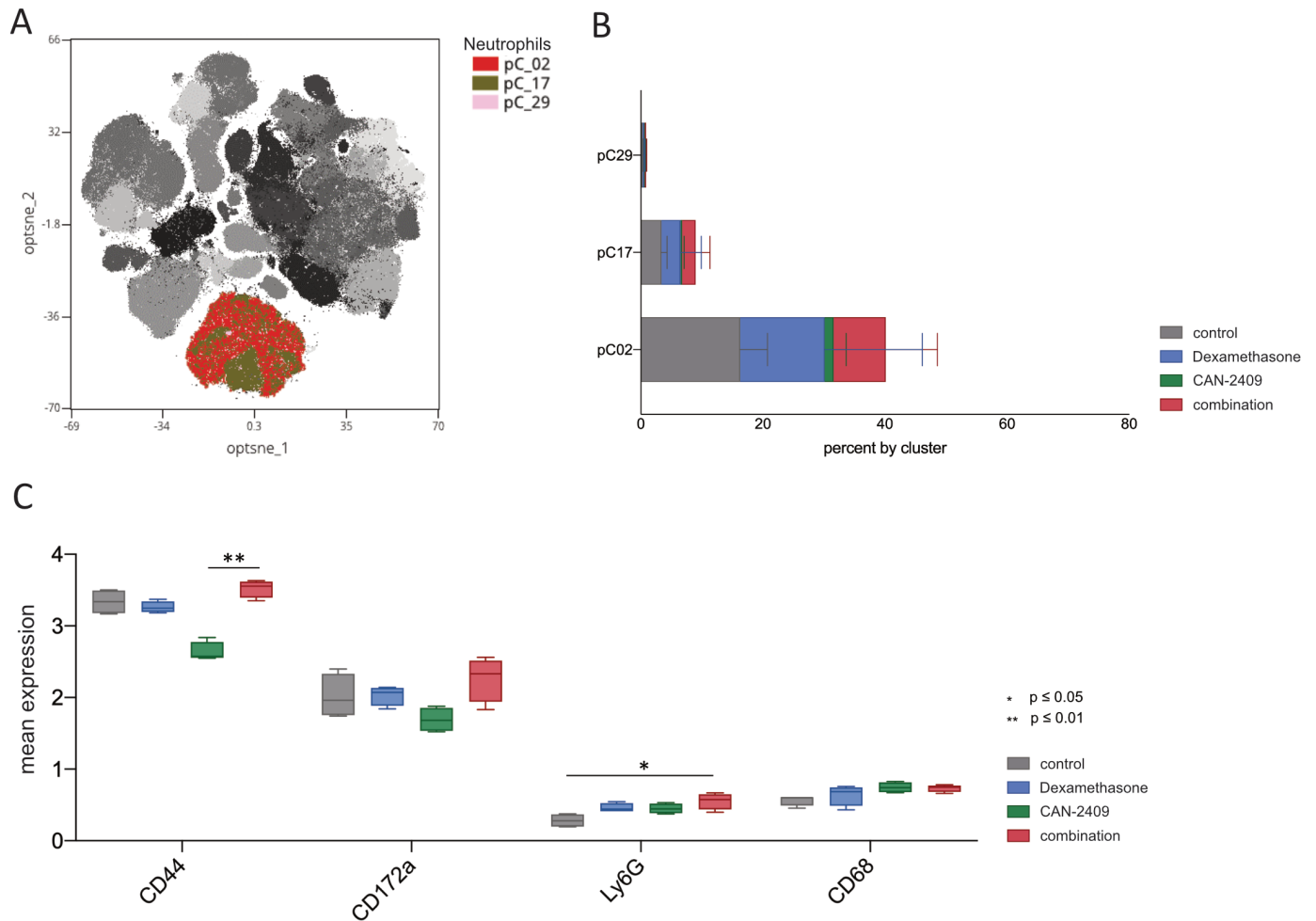


Figure 6 Increased neutrophil count and activation profile after treatment with dexamethasone \pm CAN-2409. (A) Overlay of leukocyte clusters on tSNE plot with focus on neutrophils. Cluster of interest for neutrophils are pC02, pC17, and pC29. (B) Cluster distribution of the neutrophil population in relation to therapy. Dexamethasone and combination treatment is associated with an increase in the neutrophil cell population in all clusters (bars show mean \pm SD). (C) Expression of significantly altered markers on macrophages. Combinatorial treatment with CAN-2409 and dexamethasone is associated with increased median expression of CD44, Ly6G, CD172a and CD68 with CD44 (adj. $p=0.004$) being significantly upregulated in combination versus CAN_2409 and Ly6G (adj. $p=0.015$) being significantly upregulated in the combination group compared with control.

figure S4A). A similar pattern of marker expression was observed in the majority of macrophage clusters. SAM revealed significant expression changes in CD44, CD172a, and CD196 expressions across the macrophage populations (figure 5C) with CD172a being also significantly overexpressed as measured with Kruskal-Wallis test in the combination cohort compared with control. As shown in figure 4, all markers showed the highest expression in the combination treatment groups.

Enhanced neutrophil counts in the tumor microenvironment facilitate the growth of GBM initiating cells,⁴⁰ and activated neutrophils are correlated with accelerated tumor progression.⁴¹ Figure 3 shows that CAN-2409 treatment leads to a pronounced decrease in neutrophil levels. Three neutrophil clusters were identified, pC0₂ being the most prominent and it is greatly reduced post-CAN-2409 treatment. SAM showed significant elevation of CD44, CD172a, and Ly6G in the combination group with CD44 and Ly6G being also significantly elevated in

consecutive testing with the Kruskal-Wallis test. CD68 was increased by CAN-2409 treatment (figure 6A–C).

All in all, it remains to state that combined treatment with CAN-2409 and dexamethasone has a profound effect on the innate immune cell population with significant overexpression of CD17a in macrophages and of CD44 and Ly6G in neutrophils.

DISCUSSION

Dexamethasone is frequently used in the symptomatic treatment of GBM to relieve edema. However, available data suggest that dexamethasone ultimately may have a negative impact on survival, as observed in a multicenter retrospective clinical data analysis.¹⁰ Intratumoral immunotherapies are under investigation for various cancers, including GBM, but the effects of dexamethasone in this context have not been investigated before.

In the present study, we evaluated the effects of continuous high-dose dexamethasone treatment during prototypic oncolytic viral immunotherapy, CAN-2409 treatment, in a mouse model of GBM. CAN-2409 treatment is an investigational therapy under clinical development for GBM. It induces a local immune response against a range of cancer neoantigens, followed by a systemic immune response. The data presented here suggest that high-dose dexamethasone may abrogate the antitumorigenic effects of CAN-2409 treatment by reducing the subsequent immune response.

A limitation of our *in vitro* study is that we could not capture the full scope of the mechanism of action of CAN-2409 treatment *in vivo*, as this involves effects on cell migration, cell retention, and cell activation in the tissue. In addition, in our *in vivo* experiments, we used high-dose dexamethasone (starting dose resulting in serum levels that are significantly higher than those achieved in human patients treated with 4×4mg dexamethasone) for 7 days, but in accordance with the dose used in other publications.¹⁴ In contrast to the results shown by Iorgulescu *et al*, we saw a significantly prolonged survival of dexamethasone-treated animals compared with control. Dexamethasone is known for promoting weight gain also in rodents⁴²; therefore, the murine survival study end-point criteria ‘weight loss’ might confer a bias in this regard. To better mimic the clinical situation with high tumor cell burden in which patients usually receive dexamethasone, treatment was started on day 9 after tumor implantation, therefore varying the treatment settings from previous reports.²¹ This explains the variation in treatment efficacy of CAN-2409 in comparison to preceding studies.

Despite the limitations of this preclinical study, the data are consistent with previous work, showing the profound effects of high-dose corticosteroids on the human immune system.⁴³ Together, these data suggest that concurrent high-dose dexamethasone treatment could potentially impair the efficacy of oncolytic viral immunotherapy (or other immunotherapies) of GBM. Our findings support the rationale for future studies in patients, addressing the question which dosing regimen of dexamethasone may provide an optimal balance between immediate symptom control and ultimate outcome.

The effect of dexamethasone treatment may be dependent on the specific treatments administered to the patient with GBM. For example, dexamethasone treatment may reduce the proapoptotic effects of temozolomide in U87MG and T98G cell lines as well as GSCs.^{44–46} In radiotherapy, dexamethasone was reported to radiosensitize astrocytoma cell lines by increasing oxidative stress⁴⁷ and reducing dispersal and growth,⁴⁸ although other studies could not reproduce these findings.^{49–50} Recent studies have shown that dexamethasone has an adverse influence on the efficacy of systemic immune checkpoint blockade in murine GBM models as well as in patients with GBM,¹⁴ in line with our findings for intratumoral immunotherapy.

Our data support the notion that dexamethasone may impact the effectiveness of local immunotherapies due to its profound immunosuppressive effects. A dexamethasone-mediated disruption of the bystander effect of CN-2409 also has to be considered as playing a crucial role in this regard.⁵¹ Also, pre-existing immunity against therapeutic virotherapies may also have an impact on local immunotherapies.⁵²

Cell viability and T-cell killing assays have shown that dexamethasone diminishes the effects of CAN-2409 treatment *in vitro*, with immune-mediated killing being the most affected. *In vivo*, dexamethasone in combination with CAN-2409 results in reduced median survival compared with CAN-2409 treatment alone. We found that CAN-2409 treatment alone leads to increased proportions of CD8⁺ T cells, CD4⁺ T cells, and B cells with a reduction in neutrophils and macrophages, with dexamethasone showing opposite effects. Interestingly, Treg proportions were reduced by dexamethasone treatment and nearly undetectable in the combination treatment group. Previous studies on the effects of steroids on Tregs have produced contradictory results. One study showed that dexamethasone may induce apoptosis in FOXP3⁺–CD4⁺–T cells. Treg numbers were significantly decreased after combination treatment.⁵³ However, their function may be increased as suggested by higher CD44 expression.⁵⁴ CD44 functions as an enhancer of Treg-associated immunosuppressive effects, including IL-10 production.⁵⁵ Also, cell survival of CD4⁺ T cells might be reduced as Ly6C⁺⁵⁶ and CD39 surface expression is amplified.⁵⁷ These observations coincide with upregulation of I-A/I-E/MHC II, thereby conveying that especially antigen-presenting cells (APCs) might be affected by the aforementioned changes. These alterations merit further detailed analysis in future studies.

Our CyTOF analyses suggest that the CAN-2409-mediated reduction in neutrophil numbers is blocked by treatment with dexamethasone (figure 3) together with an increase in the protumorigenic markers CD172a and Ly6C,^{58–59} pointing to an even further reduced antitumor immunity. Neutrophils in the GBM microenvironment are considered tumor-promoting as their presence is associated with mesenchymal tumor characteristics and facilitates the growth of GSCs.⁴⁰

The GBM microenvironment is characterized by infiltration of macrophages, which may have protumorigenic, immunosuppressive properties.⁶⁰ Our data show that treatment with high-dose dexamethasone alone and in combination with CAN-2409 treatment may lead to an increase in macrophages and concomitant overexpression of CD172a. CD172a/SIRPα binding to its ligand CD47 prevents phagocytosis of cancer cells⁶¹ and has been shown to augment antineoplastic effects of innate immune cells.⁵⁸ The relevance of increased CD44 and CD196/CCR6 expression on macrophages after the combination therapy remains uncertain at this point. However, current data implicate protumorigenic effects of the CCR6-CCL20 pathway.⁶²

Taken together, our findings as well as those of others highlight that dexamethasone has the potential to interfere with multiple facets of GBM therapy, ranging from radiochemotherapy to immunotherapy. This clinical problem could be addressed by limiting the use of dexamethasone to the absolute necessary minimum or to assess pharmacological alternatives for antiedema treatment. To this end, the anti-VEGF-antibody bevacizumab and corticorelin acetate have been suggested as options to replace dexamethasone,⁹ but neither are routinely administered for that purpose yet.

We conclude that concurrent continuous use of high-dose dexamethasone may interfere with locally delivered immunotherapy. Thus, corticosteroids as a supportive treatment for GBM in conjunction with immunotherapies should require careful consideration and should be as limited as possible. Further studies to identify efficient alternatives or combinatorial treatments to counterbalance dexamethasone's immunosuppressive effect are warranted.

Twitter Alec M Griffith @AlecAsks

Acknowledgements The authors thank Candel Therapeutics (Needham, MA, USA) for providing CAN-2409 and Ganciclovir used in this study.

Contributors Conceptualization: MSK, SL, and EA. Methodology: MSK, MZ, AMG, MON, EA, SL, and JAL. Investigation: MSK, SL, and EA. Visualization: MSK and AMG. Funding acquisition: SL, EA, and JAL. Project administration: MSK, SL, and EA. Supervision: SL, EA, and JAL. Writing, original draft: MSK and SL. Writing, review and editing: MSK, SL, EA, MZ, MON, AMG, JAL, GT, PPT, FB, EA, LKA, and BWG. Guarantor: SEL

Funding This study was funded by NCI P01CA069246. This research was partially funded by NCI R50 CA243706-02 (MON) and Else Kröner Fresenius Forschungskolleg (2015_Kolleg_14) (GT).

Competing interests None declared.

Patient consent for publication Not applicable.

Ethics approval This study does not involve human participants.

Provenance and peer review Not commissioned; externally peer reviewed.

Data availability statement Data are available upon reasonable request. All data relevant to the study are included in the article or uploaded as supplementary information. Contact: sean_lawler@brown.edu.

Supplemental material This content has been supplied by the author(s). It has not been vetted by BMJ Publishing Group Limited (BMJ) and may not have been peer-reviewed. Any opinions or recommendations discussed are solely those of the author(s) and are not endorsed by BMJ. BMJ disclaims all liability and responsibility arising from any reliance placed on the content. Where the content includes any translated material, BMJ does not warrant the accuracy and reliability of the translations (including but not limited to local regulations, clinical guidelines, terminology, drug names and drug dosages), and is not responsible for any error and/or omissions arising from translation and adaptation or otherwise.

Open access This is an open access article distributed in accordance with the Creative Commons Attribution Non Commercial (CC BY-NC 4.0) license, which permits others to distribute, remix, adapt, build upon this work non-commercially, and license their derivative works on different terms, provided the original work is properly cited, appropriate credit is given, any changes made indicated, and the use is non-commercial. See <http://creativecommons.org/licenses/by-nc/4.0/>.

ORCID iDs

Marilyn S Koch <http://orcid.org/0000-0002-8335-3543>

Alec M Griffith <http://orcid.org/0000-0002-4289-3017>

REFERENCES

- Stupp R, Mason WP, van den Bent MJ, *et al.* Radiotherapy plus concomitant and adjuvant temozolomide for glioblastoma. *N Engl J Med* 2005;352:987–96.
- Omuro A, Vlahovic G, Lim M, *et al.* Nivolumab with or without ipilimumab in patients with recurrent glioblastoma: results from exploratory phase I cohorts of CheckMate 143. *Neuro Oncol* 2018;20:674–86.
- Hilf N, Kuttruff-Coqui S, Frenzel K, *et al.* Actively personalized vaccination trial for newly diagnosed glioblastoma. *Nature* 2019;565:240–5.
- Brown CE, Alizadeh D, Starr R, *et al.* Regression of glioblastoma after chimeric antigen receptor T-cell therapy. *N Engl J Med Overseas Ed* 2016;375:2561–9.
- Chiocca EA, Nassiri F, Wang J, *et al.* Viral and other therapies for recurrent glioblastoma: is a 24-month durable response unusual? *Neuro Oncol* 2019;21:14–25.
- Wheeler LA, Manzanera AG, Bell SD, *et al.* Phase II multicenter study of gene-mediated cytotoxic immunotherapy as adjuvant to surgical resection for newly diagnosed malignant glioma. *Neuro Oncol* 2016;18:1137–45.
- Berger G, Marloye M, Lawler SE. Pharmacological modulation of the sting pathway for cancer immunotherapy. *Trends Mol Med* 2019;25:412–27.
- Giles AJ, Hutchinson M-KND, Sonnemann HM, *et al.* Dexamethasone-Induced immunosuppression: mechanisms and implications for immunotherapy. *J Immunother Cancer* 2018;6:1–13.
- Arvold ND, Armstrong TS, Warren KE, *et al.* Corticosteroid use endpoints in neuro-oncology: response assessment in neuro-oncology Working group. *Neuro Oncol* 2018;20:897–906.
- Pitter KL, Tamagno I, Alikhanyan K, *et al.* Corticosteroids compromise survival in glioblastoma. *Brain* 2016;139:1458–71.
- Shields LBE, Shelton BJ, Shearer AJ, *et al.* Dexamethasone administration during definitive radiation and temozolomide renders a poor prognosis in a retrospective analysis of newly diagnosed glioblastoma patients. *Radiat Oncol* 2015;10.
- Wong ET, Lok E, Gautam S, *et al.* Dexamethasone exerts profound immunologic interference on treatment efficacy for recurrent glioblastoma. *Br J Cancer* 2015;113:232–41.
- Keskin DB, Anandappa AJ, Sun J, *et al.* Neoantigen vaccine generates intratumoral T cell responses in phase Ib glioblastoma trial. *Nature* 2019;565:234–9.
- Iorgulescu JB, Gokhale PC, Speranza MC, *et al.* Concurrent dexamethasone limits the clinical benefit of immune checkpoint blockade in glioblastoma. *Clin Cancer Res* 2021;27:276–87.
- Vile RG, Nelson JA, Castleden S, *et al.* Systemic gene therapy of murine melanoma using tissue specific expression of the HSVtk gene involves an immune component. *Cancer Res* 1994;54:6228–34.
- Kleijn A, Kloezeman J, Treffers-Westerlaken E, *et al.* The in vivo therapeutic efficacy of the oncolytic adenovirus Delta24-RGD is mediated by tumor-specific immunity. *PLoS One* 2014;9:e97495.
- Vile RG, Castleden S, Marshall J, *et al.* Generation of an anti-tumour immune response in a non-immunogenic tumour: HSVtk killing in vivo stimulates a mononuclear cell infiltrate and a Th1-like profile of intratumoural cytokine expression. *Int J Cancer* 1997;71:267–74.
- Krohne TU, Shankara S, Geissler M, *et al.* Mechanisms of cell death induced by suicide genes encoding purine nucleoside phosphorylase and thymidine kinase in human hepatocellular carcinoma cells in vitro. *Hepatology* 2001;34:511–8.
- Williams SP, Nowicki MO, Liu F, *et al.* Irinotecan decrease glioma invasion by blocking migratory phenotypes in both the tumor and stromal endothelial cell compartments. *Cancer Res* 2011;71:5374–80.
- Van Brocklyn J, Bremer EG, Yates AJ. Gangliosides inhibit platelet-derived growth factor-stimulated receptor dimerization in human glioma U-1242MG and Swiss 3T3 cells. *J Neurochem* 1993;61:371–4.
- Speranza M, Passaro C, Riclefs F. Neuro-oncology cytotoxic immunotherapy and immune checkpoint blockade in glioblastoma. *Neuro Oncol* 2018;20:225–35.
- Charan J, Kantharia ND. How to calculate sample size in animal studies? *J Pharmacol Pharmacother* 2013;4:303–6.
- Finck R, Simonds EF, Jager A, *et al.* Normalization of mass cytometry data with bead standards. *Cytometry A* 2013;83:483–94.
- Chevrier S, Crowell HL, Zanutelli VRT, *et al.* Compensation of signal spillover in suspension and imaging mass cytometry. *Cell Syst* 2018;6:612–20.
- Zunder ER, Finck R, Behbehani GK, *et al.* Palladium-based mass tag cell barcoding with a doublet-filtering scheme and single-cell deconvolution algorithm. *Nat Protoc* 2015;10:316–33.

- 26 Belkina AC, Ciccolella CO, Anno R, *et al.* Automated optimized parameters for T-distributed stochastic neighbor embedding improve visualization and analysis of large datasets. *Nat Commun* 2019;10:1–12.
- 27 Stassen SV, Siu DMD, Lee KCM, *et al.* PARC: ultrafast and accurate clustering of phenotypic data of millions of single cells. *Bioinformatics* 2020;36:2778–86.
- 28 Chu G, Li J, Narasimhan B. SAM - significance analysis of microarrays - users guide and technical document. *Policy* 2011:1–42.
- 29 Liu Q, Muruve DA. Molecular basis of the inflammatory response to adenovirus vectors. *Gene Ther* 2003;10:935–40.
- 30 Chhikara M, Huang H, Vlachaki MT, *et al.* Enhanced therapeutic effect of HSV-tk+GCV gene therapy and ionizing radiation for prostate cancer. *Mol Ther* 2001;3:536–42.
- 31 Predina JD, Haas AR, Martinez M, *et al.* Neoadjuvant Gene-Mediated cytotoxic immunotherapy for non-small-cell lung cancer: safety and immunologic activity. *Mol Ther* 2021;29:658–70.
- 32 Badie B, Schartner JM, Paul J, *et al.* Dexamethasone-Induced abolition of the inflammatory response in an experimental glioma model: a flow cytometry study. *J Neurosurg* 2000;93:634–9.
- 33 Urban SL, Berg LJ, Welsh RM. Type 1 interferon licenses naïve CD8 T cells to mediate anti-viral cytotoxicity. *Virology* 2016;493:52–9.
- 34 Schuler PJ, Saze Z, Hong C-S, *et al.* Human CD4+ CD39+ regulatory T cells produce adenosine upon co-expression of surface CD73 or contact with CD73+ exosomes or CD73+ cells. *Clin Exp Immunol* 2014;177:531–43.
- 35 Ziegler SF, Ramsdell F, Alderson MR. The activation antigen CD69. *Stem Cells* 1994;12:456–65.
- 36 Jeannin P, Herbault N, Delneste Y, *et al.* Human effector memory T cells express CD86: a functional role in naïve T cell priming. *J Immunol* 1999;162:2044–8.
- 37 Brochez L, Meireson A, Chevolet I, *et al.* Challenging PD-L1 expressing cytotoxic T cells as a predictor for response to immunotherapy in melanoma. *Nat Commun* 2018;9:2921.
- 38 Diskin B, Adam S, Cassini MF, *et al.* Pd-L1 engagement on T cells promotes self-tolerance and suppression of neighboring macrophages and effector T cells in cancer. *Nat Immunol* 2020;21:442–54.
- 39 Johnson RMG, Wen T, Dong H. Bidirectional signals of PD-L1 in T cells that fraternize with cancer cells. *Nat Immunol* 2020;21:365–6.
- 40 Liang J, Piao Y, Holmes L, *et al.* Neutrophils promote the malignant glioma phenotype through S100A4. *Clin Cancer Res* 2014;20:187–98.
- 41 Rahbar A, Cederarv M, Wolmer-Solberg N, *et al.* Enhanced neutrophil activity is associated with shorter time to tumor progression in glioblastoma patients. *Oncimmunology* 2016;5:e1075693.
- 42 Veyrat-Durebex C, Deblon N, Caillon A, *et al.* Central glucocorticoid administration promotes weight gain and increased 11 β -hydroxysteroid dehydrogenase type 1 expression in white adipose tissue. *PLoS One* 2012;7:34002.
- 43 Gerlag DM, Haringman JJ, Smeets TJM, *et al.* Effects of oral prednisolone on biomarkers in synovial tissue and clinical improvement in rheumatoid arthritis. *Arthritis Rheum* 2004;50:3783–91.
- 44 Sur P, Sribnick EA, Patel SJ, *et al.* Dexamethasone decreases temozolomide-induced apoptosis in human glioblastoma T98G cells. *Glia* 2005;50:160–7.
- 45 Das A, Banik NL, Patel SJ, *et al.* Dexamethasone protected human glioblastoma U87MG cells from temozolomide induced apoptosis by maintaining Bax:Bcl-2 ratio and preventing proteolytic activities. *Mol Cancer* 2004;3:36.
- 46 Luedi MM, Singh SK, Mosley JC, *et al.* A dexamethasone-regulated gene signature is prognostic for poor survival in glioblastoma patients. *J Neurosurg Anesthesiol* 2017;29:46–58.
- 47 Ortega-Martínez S. Dexamethasone acts as a radiosensitizer in three astrocytoma cell lines via oxidative stress. *Redox Biol* 2015;5:388–97.
- 48 Shannon S, Vaca C, Jia D, *et al.* Dexamethasone-Mediated activation of fibronectin matrix assembly reduces dispersal of primary human glioblastoma cells. *PLoS One* 2015;10:e0135951.
- 49 Mariotta M, Perewusnyk G, Koechli OR, *et al.* Dexamethasone-Induced enhancement of resistance to ionizing radiation and chemotherapeutic agents in human tumor cells. *Strahlentherapie und Onkologie* 1999;175:392–6.
- 50 Komakech A, Im J-H, Gwak H-S, *et al.* Dexamethasone interferes with autophagy and affects cell survival in irradiated malignant glioma cells. *J Korean Neurosurg Soc* 2020;63:566–78.
- 51 Robe PA, Nguyen-Khac M, Jolois O, *et al.* Dexamethasone inhibits the HSV-tk/ ganciclovir bystander effect in malignant glioma cells. *BMC Cancer* 2005;5:32.
- 52 Delman KA, Bennett JJ, Zager JS, *et al.* Effects of preexisting immunity on the response to herpes simplex-based oncolytic viral therapy. *Hum Gene Ther* 2000;11:2465–72.
- 53 Pandolfi J, Baz P, Fernández P, *et al.* Regulatory and effector T-cells are differentially modulated by dexamethasone. *Clin Immunol* 2013;149:400–10.
- 54 Liu T, Soong L, Liu G, *et al.* Cd44 expression positively correlates with FOXP3 expression and suppressive function of CD4+Treg cells. *Biol Direct* 2009;4:40.
- 55 Bollyky PL, Falk BA, Long SA, *et al.* Cd44 costimulation promotes FOXP3 + regulatory T cell persistence and function via production of IL-2, IL-10, and TGF- β . *J Immunol* 2009;183:2232–41.
- 56 Marshall HD, Chande A, Jung YW, *et al.* Differential expression of Ly6C and T-bet distinguish effector and memory Th1 CD4+ cell properties during viral infection. *Immunity* 2011;35:633–46.
- 57 Fang F, Yu M, Cavanagh MM, *et al.* Expression of CD39 on activated T cells impairs their survival in older individuals. *Cell Rep* 2016;14:1218–31.
- 58 Ring NG, Herndler-Brandstetter D, Weiskopf K. Anti-SIRP α antibody immunotherapy enhances neutrophil and macrophage antitumor activity.
- 59 Spiegel A, Brooks MW, Houshyar S, *et al.* Neutrophils suppress intraluminal NK cell-mediated tumor cell clearance and enhance extravasation of disseminated carcinoma cells. *Cancer Discov* 2016;6:630–49.
- 60 Grégoire H, Roncali L, Rousseau A, *et al.* Targeting tumor associated macrophages to overcome conventional treatment resistance in glioblastoma. *Front Pharmacol* 2020;11:368.
- 61 Takahashi S. Molecular functions of SIRP α and its role in cancer (review). *Biomed Reports* 2018;9:3–7.
- 62 Kadomoto S, Izumi K, Mizokami A. The CCL20-CCR6 axis in cancer progression. *Int J Mol Sci* 2020;21:5186–18.